Smart Transformer for the Provision of Coordinated Voltage and Frequency Support in the Grid

Junru Chen[1], Rongwu Zhu[2], Muyang Liu[1], Giovanni De Carne[2],
Marco Liserre[2], Federico Milano[1], Terence O'Donnell[1]

1. University College Dublin, Dublin, Ireland
2. Christian-Albrechts-Universität zu Kiel, Kiel, Germany
Junru.chen.1@ucdconnect.ie

***Abstract*—Considering the increase in renewable generation and the consequent reduction in power system inertia, the Virtual Synchronous Machine (VSM) control method has been proposed to control power electronics converters to emulate the inertia and other the characteristics of the synchronous machine. However, to achieve the function of VSM control, an extra energy base, typically storage, is required to connect to the controlled converter. In this work we investigate the application of the VSM control to the distribution system demand through the use of a VSM controlled smart transformer. Through control of the demand in this way, the demand itself can be used to emulate inertia and provide frequency support. This paper presents the details of the flexible demand control applied to a smart transformer supplying a low voltage distribution grid. The operation of the control is validated on scaled hardware using real time simulation with hardware in the loop. Simulations on a 400 kVA, 400 V distribution network are used to quantify the demand flexible. IEEE 39 bus is used to verify the benefit of the proposed control in terms of voltage and frequency in the power system.**

Keywords—Smart transformer, virtual synchronous machine, virtual inertia, frequency support, voltage support

I. INTRODUCTION

The increase in power electronics interfaced renewable generation and consequent displacement of conventional synchronous generation is leading to a reduction in the inertia of the power system. This reduction is a potential risk to power system transient stability. Thus, with the increasing use of renewables, the power system should be more flexible to maintain stability, i.e. supplying frequency and voltage support from alternative sources such as storage and renewable generation. Power electronics connected renewable generation could mimic some of the properties of synchronous generation and thus provide power system support, e.g Beck and Hesse proposed the Virtual Synchronous Machine (VSM) method in 2007. The VSM method controls the converter to mimic the synchronous generator, in order to increase the system inertia and support the system frequency [1]. Different VSM implementations have already been proposed, e.g. the virtual synchronous generator based on synchronous-dq-frame [2-3], the synchronverter based on vector control [4], and other types based on outer power, inner current control [5]. Although these methods can be embedded into wind turbine systems [6] and PV systems [7], electric energy storage, i.e. super-capacitor or battery, is required to be connected to the DC port of the converter, in order to provide the droop power and virtual kinetic energy.

The VSM is usually proposed to be used in the supply side to provide frequency and voltage support. On the other hand, the power system demand can be controlled through control of the voltage, as is used in conservation voltage reduction (CVR). Meanwhile smart transformers (ST) have been proposed as a replacement for the conventional transformer in the distribution system for its advantages in terms of flexible control and renewables integration [8]. The voltage and frequency of the ST connected distribution system is fully controllable by the ST. Thus, potentially the demand is controllable within limits assuming that the load type is known. The traditional transformer equipped with a tap changer has often been used to implement conservation voltage reduction to purposely reduce the demand in the peak-time by the means of voltage reduction. However since it typically lacks the means of dynamically identifying the load type the method relies on load forecasting and historical data to determine voltage reduction, and moreover only reduces the voltage in limited steps due to the mechanical tap changer action. In this work we investigate how a smart power electronics transformer can be used to dynamically control demand as virtual kinetic energy in VSM to support voltage and frequency in the utility grid.

The provision of voltage support to the transmission system from an ST has previously been reported in [9]. A means of load identification which could be used with an ST fed distribution system has been proposed in [10]. In addition reference [11] proposed a method for dynamic voltage regulation by ST to minimize the demand and [12] proposed the demand control to limit overload of ST. However to the authors knowledge no previous work has investigated the possibility of providing grid frequency support from an ST by dynamic control of the demand by means of the ST voltage. This work describes the implementation of VSM control into ST to provide grid frequency support by means of regulating the distribution system demand and voltage support by means of controlled reactive power compensation. The proposed method in the paper is called flexible demand control.

The paper is organized as follows: Section II introduces the implementation method of the flexible demand control in the ST including its hardware in the loop validation. Section III statistically analyzes the benefit from proposed control by taking a 400 kVA, 400 V distribution network into account.

Section IV provides the closed loop simulation in transmission level using the IEEE 39-bus standard system as an example, while section V draws the conclusions.

II. Flexible Demand Control

Commonly suggested topologies for the ST include a DC-DC link in the structure and a voltage controlled converter on the rectifier (Medium Voltage) side and inverter (Low voltage) side, as shown in Fig. 1. The rectifier stage is controlled as the conventional current-mode, power controller, maintaining the MVDC voltage with a PLL to achieve MV grid synchronization. The DC/DC stage regulates the LVDC voltage, while the inverter stage actively controls the LVAC voltage and frequency to the distribution system.

One advantage of this ST topology is that only the active power passes from the MV side to LV side while reactive power is decoupled. Based on this characteristic, the flexible demand control in ST can support voltage by implementing reactive power-voltage droop in the rectifier control system, while supporting frequency by controlling distribution system demand from voltage regulation in the inverter control system.

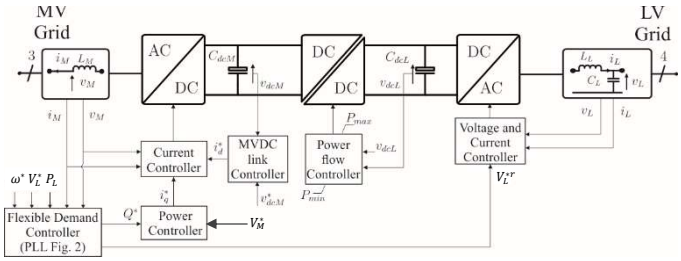

Fig. 1. Flexible demand controlled ST system

A. Flexible Demand Control

It has previously been shown how frequency support could be provided from grid tied converters by making use of the PLL to emulate swing equation dynamics [13]. A similar approach is followed here. The details of the PLL implementation and computation of references for the control is illustrated in Fig. 2. The PLL on the rectifier side measures the grid frequency and voltage, where specifically, V_d contains voltage information, while V_q contains phase information.

The frequency support control has two steps. In the first step a load identification is performed which is used to identify the demand voltage sensitivity S_V in Fig. 2. In the second step the output voltage is controlled according to the frequency or V_q. The load identification step is only performed when the demand undergoes a significant change [11], otherwise, the control continues to work in the second step-frequency support function as shown in Fig. 2.

The voltage sensitivity (S_V) is defined as the percentage of power reduction resulting from an intentional 1% voltage reduction as in (1), where ΔV is the percentage of intentional voltage change, ΔP is the percentage of measured power change. Therefore, when $S_V > 0$, it means voltage reduction results in the demand reduction, and when $S_V < 0$, it means voltage increase results in the demand reduction. This opposite relationship is represented by the voltage sensitivity block in Fig. 2.

$$S_V = \frac{\Delta \mathrm{P}}{\Delta \mathrm{V}} \tag{1}$$

The frequency and rate of change of frequency signals for the flexible demand control are obtained from the PLL (see Fig. 2). Consider that initially, the PCC voltage has phase θ_0 with nominal frequency ω_0, and the PLL is synchronized with the detected phase $\theta_{g0} = \omega_0 t + \theta_0$, then:

$$V_q = V_M \sin\left(\omega_0 t + \theta_0 - \theta_{g0}\right) = 0 \tag{2}$$

At the instant of a frequency event in the grid which for example causes a ramp change in frequency where the grid frequency ω_g changes with slope $\Delta\dot{\omega}_g$, while the PLL has not responded, then:

$$\begin{aligned} V_q &= V_M \sin\left(\left(\omega_0 + \Delta\dot{\omega}_g t\right)t + \theta_0 - \theta_{g0}\right) \\ &= V_M\left(\left(\omega_0 + \Delta\dot{\omega}_g t\right)t + \theta_0 - \theta_{g0}\right) \\ &= V_M \Delta\dot{\omega}_g t^2 \end{aligned} \tag{3}$$

In order to regulate V_q to 0 or re-lock the phase, the PLL will move its detected phase θ_g to ($\theta_{g0} + \Delta\dot{\omega}_g t^2$), then:

$$\theta_g = \theta_{g0} + \Delta\dot{\omega}_g t^2 = \theta_{g0} + K \iint \Delta\dot{\omega}_g \tag{4}$$

Thus, in order to achieve zero steady state error, any type of PLL requires two integrators in the control loop. Besides, a compensator H(s) (embedded in K in (4)) is also typically required to eliminate the harmonics. Then, the signal after the compensator H(s) in Fig. 2 mainly contains the grid $\Delta\dot{\omega}_g$ or rate of change of frequency (RoCoF) information and some unfiltered harmonics. The RoCoF gain K_t is used to proportionally change the inverter voltage according to the RoCoF. The frequency deviation $\Delta\omega_g$ obtained after the integrator, provides a frequency droop term with gain K_d. The frequency droop term and RoCoF term sum up to determine the ST inverter output voltage (distribution system supply voltage) reference V_L^{*r}.

$$V_L^{*r} = \frac{-S_V}{|S_V|}\left(K_t \frac{\Delta\omega_g}{\Delta t} + K_d \cdot \Delta\omega_g\right) + V_L^* \tag{5}$$

Where V_L^* is the nominal voltage. Note that equation (5) has a similar structure to the swing equation. The varied demand ΔP_L resulting from the voltage change and used to support frequency can be estimated from (6), where $P_{L,0}$ is the active power demand at nominal supply voltage.

$$\Delta P_L = -S_V P_{L,0}\left(K_t \frac{\Delta\omega_g}{\Delta t} + K_d \cdot \Delta\omega_g\right) \tag{6}$$

Note, that in order to satisfy typical distribution system constraints, i.e. EN 50160, the output voltage is limited to be within the range of $(V_L^* \pm 0.1)\ pu$ [14]. Then, the available active power $\Delta P_{L,max}$ available to support frequency is:

$$\Delta P_{L,max} = S_V P_0 \frac{V_L^* - V_{Lm}}{V_L^*} \tag{7}$$

Where V_{Lm} is the maximum or minimum voltage output to this distribution system.

The voltage support for the MV side uses a voltage-to-reactive power droop control as in (8).

$$Q^* = K_q(V_M^* - V_d) + Q_0 \tag{8}$$

Where K_Q is the voltage-to-reactive power droop gain, Q_0 is the initial reactive power output to transmission system, Q^* is the controlled reactive power output.

The maximum reactive power compensation is limited by the rating of the ST rectifier, S_{ST} and the active power demand of the load P_L in the distribution system. Thus (ignoring losses in the ST):

$$Q_{ST,max} = \pm\sqrt{S_{ST}^2 - P_L^2} \tag{9}$$

$$P_L = P_{L,0} + \Delta P_L \tag{10}$$

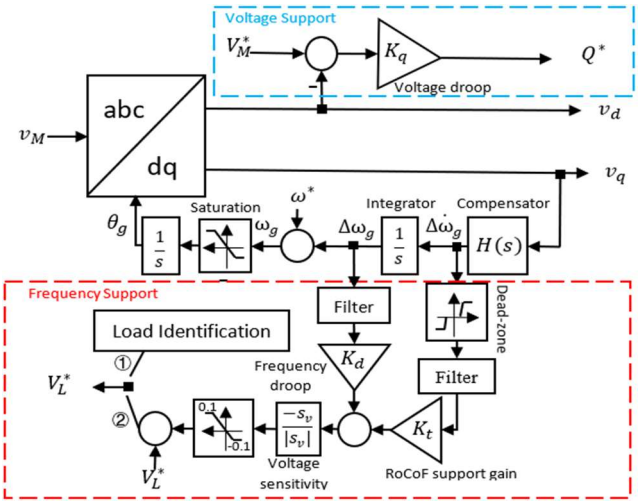

Fig. 2. Phase locked loop embedded flexible demand control

With reference to Fig. 1, based on a voltage measurement from the PLL, a drooped reactive power reference Q^* is calculated for the voltage support (8), and is provided to the outer power, inner current control of the rectifier. Based on a measurement of frequency from the PLL, a voltage reference for the frequency support is computed from (5) and passed to the outer voltage, inner current control for the inverter side. Consequently, the load power can be varied in a range (7), depending on the load type and this power range can be used to compensate the supply-demand mismatch, i.e. provide frequency support.

B. Parameter selection

Grid codes usually specify parameters for frequency support from generators. For example, in Ireland, the grid code [15] stipulates that the active power control should have a deadband of ±0.5 Hz for wind farm power station. If the transmission system frequency excursion outside these range, the active power controller shall provide at least 60% of its expected additional active power within 5 s, and 100% within 15 s. When the frequency below 48 Hz or above 52 Hz, the controlled device shall inject or absorb maximum active power respectively. Meanwhile, the current grid code in Ireland [16] only requires generators to be able to ride through RoCoF of 0.5 Hz/s. Considering these standards, the demand supply voltage should be controlled to the extremum when either the frequency deviation is 2 Hz (0.04 pu) or the RoCof is 0.5 Hz/s (0.01 pu/s). Thus:

$$\begin{cases} K_d = \dfrac{0.1\ (pu)}{0.04\ (pu)} = 2.5 \\ K_t = \dfrac{0.1\ (pu)}{0.01\ (pu/s)} = 10 \end{cases} \tag{11}$$

The time constant of inner current outer voltage control or inner current outer power control for voltage controlled converter is typically less than 10 ms. To eliminate the harmonics, the filters in the proposed control (Fig. 2) is low pass. Hence, the delay of the control is dominated by the filter. Thus, the time constant for the filter should be below 5 s. While, the deadband of $\Delta\omega_g$ is 0.5 Hz, and which of $\dot{\Delta\omega}_g$ is 0.02 Hz/s.

On the other hand, for the voltage support, for example the Irish grid code requires that the power factor shall be within 0.835 leading or lagging during continuous normal operation [17], when voltage is less than 0.1 pu deviation from nominal. Thus, K_q should be selected on the consideration of the ST reactive power (8) and the demand active power within a 0.835 power factor range for the voltage variation in normal operation i.e. 0.1 pu. i.e.:

$$0.1K_q \le \sqrt{1 - 0.835^2}P_L - Q_0 \tag{12}$$

Note, in normal operation, the reactive power compensated by the droop (8) with selected K_q (12) always satisfies the constraint (9). However, during a contingency, the MV voltage may dip below 0.9 pu, while the reactive power could continuously increase until get saturated in (9).

C. Hardware validation

The operation of the flexible demand control has been validated in scaled hardware using an OPAL-RT real time simulation with hardware in the loop. The ST is modelled as a 2 kVA back-to-back converter, where one converter is the rectifier connected to a grid emulator with adjustable voltage amplitude and frequency, while the other converter is the inverter connected to a load. The load is emulated as resistor with 163 Ω in each phase. Note, in the hardware experiment, $K_q = 53$ VA/V is chosen to significantly show the voltage-reactive power compensation.

Fig. 3 is the hardware result where the nominal phase peak voltage is 245 V and the rated frequency is 50 Hz. At 27 s, the ST inverter voltage ramps down by 1% over 2 s to identify the load. In order to validate the frequency support function, at 31 s, the transmission system frequency reduces at a rate of 1 Hz/s. In this case the load is purely resistive so that in reaction to the frequency reduction the ST output voltage reduces; at 34.5 s, the frequency goes back to 50 Hz at a rate of 0.5 Hz/s. The voltage follows this frequency rise and returns to nominal voltage in steady-state. In order to validate the voltage support function, at 38.5 s, the transmission system voltage reduces from 1 pu to 0.95 pu, the ST rectifier increases its reactive power output to support the transmission system voltage; at 40s, the grid voltage returns to nominal value, and the reactive power output consequently, returns to zero.

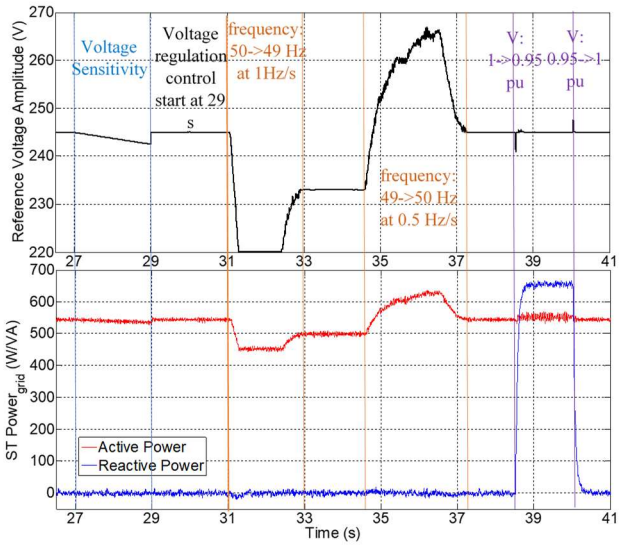

Fig. 3. Flexible demand controlled ST hardware validation result

The hardware in the loop experiment verifies the function of the proposed flexible demand control in terms of frequency to active power and grid voltage to reactive power response. However, the validation is open loop with the ST connecting to an infinite bus. The closed loop performance will be illustrated in section IV though the use of simulation.

III. Distribution System Analysis

A concern may be that the continuous voltage variation in the distribution system may cause stability problems for the loads. In order to verify the practicability of the proposed flexible demand control, we use a distribution network and its loading data in the analysis. The investigated distribution network (Fig. 4), is based on ENWL distribution grid Feeder 3 [18], and has 90 residential customers evenly distributed across three phases, with 32, 26 and 32 customers in phase A, B and C respectively. The load is modelled as residential exponential load with its loading profile at the feeder terminal shown in Fig. 5. The detail of the network and the loading profile are given in [18] and [19] respectively. The load data has 1 minute resolution and the system power flow for each 1 minute load data is solved by the Matlab EQNS function.

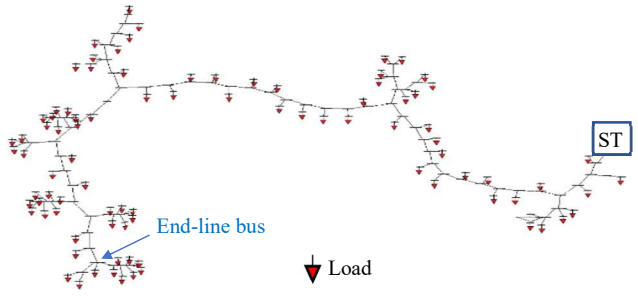

Fig. 4. Distribution system with ST

From Fig. 4, the ST is used to replace the traditional transformer as the supply to the investigated network. Due to the line impedance and its consequent voltage drop, and no distributed generation in the network, the end-line bus voltage is the minimum voltage and this end line voltage should not fall outside the range of 0.9 to 1.1 pu. Thus, as the load is constantly changing, the minimum ST inverter voltage used to support frequency in (7) is a dynamic value dependent on demand and can be determined by demand based voltage regulation method introducing in [11]. Fig. 6 displays the possible ST inverter voltage variation range for the discussed network, while, keeping the end line load voltage satisfied. Under this voltage range, the demand active power variation range is shown in Fig. 7 (a), and this available active power could be used to support the frequency is shown in Fig. 7 (b). Since the supply voltage at minimum is greater than 0.9 pu while at maximum is 1.1 pu, the available active power used for frequency increase (blue line in Fig. 7 (b)) is greater than that for frequency reduction (red line). The results indicate that for a residential load, around 5% of the loading could be used to support frequency reduction and 10% for frequency increase.

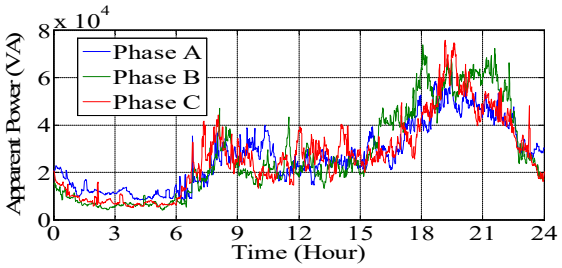

Fig. 5. Daily three phase loading profile

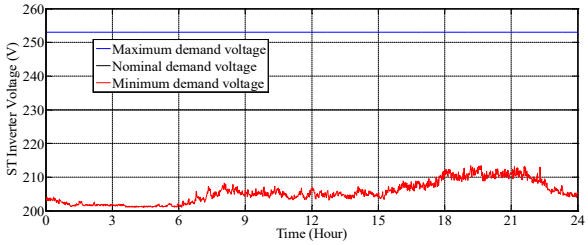

Fig. 6. Safety network supply voltage range

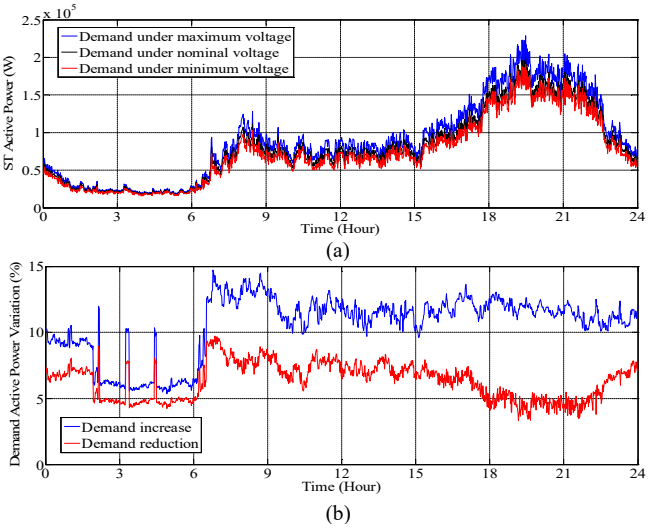

Fig. 7. Available demand active power for MV frequency support

IV. Case Study

The hardware in the loop experiment verified the function of the proposed flexible demand control in terms of frequency to active power and grid voltage to reactive power response. The distribution network analysis discussed the practicability of the control and quantified the availability of the flexible demand used in MV-grid frequency support. This section will investigate the potential effect of the proposed control in the power system through a case study based on the New England 39-bus system (Fig. 8). The synchronous generators in the system are modelled as two-axes 4th-order. Each of the generators has both primary voltage (AVR and PSS) and frequency regulators (turbine governor). Since the system is running in per unit, the ST is simplified as Back-to-Back converter with the detail of its modeling the same as in [20]. The grid connected converter is controlled as outer power inner current control with PLL as in Fig. 2, where the PLL compensator is a PI controller, while the load connected converter is controlled as outer voltage inner current control. Since the simulation does not include harmonics, the deadband and filter for flexible demand control is removed. The settings for flexible demand control is followed (11) and (12). The load connected through the ST to the bus is modelled as a static exponential load with exponent value equaling to 1.6 for active power and 3 for reactive power and with ±0.1 pu voltage variation range, while the directly connected load is modelled as constant power load since in reality, the tap-changer would keep the load constant. The case studies compare the system stability after a contingency with and without the ST with flexible demand control. The operation point for both situations initially is identical, with $P_{ST} = P_L$ and $Q_{ST} = -Q_L$ before contingency. The frequency fed to the ST is from the central of inertia, COI [21] of the power system. Simulation results in this section are obtained using Dome, a Python-based power system software tool [22]. As a contingency, the generator at bus 10 is lost at 1 s.

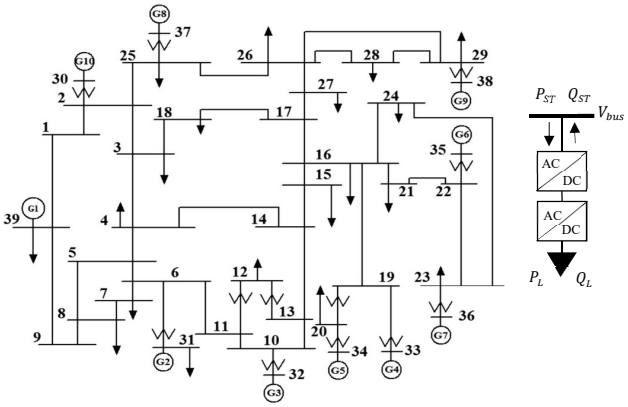

Fig. 8. New England 39-bus system & Simplified ST model

A. Scenario 1

In this scenario, we first validate the effect of the proposed flexible demand control of ST in the closed loop simulation and then analyze the system stability as the quantity of load connected through an ST with the proposed control are increased. The constant power load is replaced by the ST controlled load, in turn, from bus 3, 4, 7, 8, 12, 15, 16, 18, 20, 21, 23, 25, 26 and 27. Consequently, the ST controlled load in the system occupies from 0 up to 68.7% of the full load. There is no limit for converter power flow. Fig. 9 displays the COI frequency and bus 3 voltage under different proportions of ST controlled loads. The lowest dark line is the case without ST controlled load, while the highest red line is that with ST controlled load.

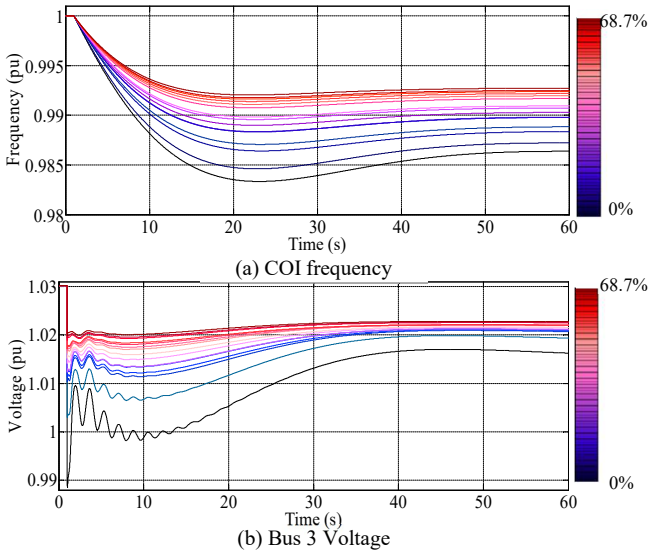

Fig. 9. Scenario 1 results, the increase proportion of the ST controlled load

From Fig. 9, the flexible demand control can support the frequency and voltage dynamically and statically. The emulated inertia K_t improves the RoCoF during the transient and the droop K_d recovers the reduced frequency in steady state. It can also be seen that the increased proportion of the ST controlled load in the system can improve the system stability in terms of both frequency and voltage.

The frequency is globally identical in transmission system, while the voltage is locally different in different buses. Thus, to investigate the voltage support for the total system, not only bus 3, Fig. 10 plots the total system voltage absolute steady state error (computed as the voltage before contingency minus the voltage after contingency in each bus as (13)) with the increase of the ST controlled load occupation. From Fig. 10, it can be seen that the increase in the proportion of ST controlled load, reduces the total steady state error, and thus indicates that the ST controlled load can help improve the total system voltage stability.

$$\text{Total steady state error} = \sum_{i=1}^{39} |V_{i,before} - V_{i,after}| \qquad (13)$$

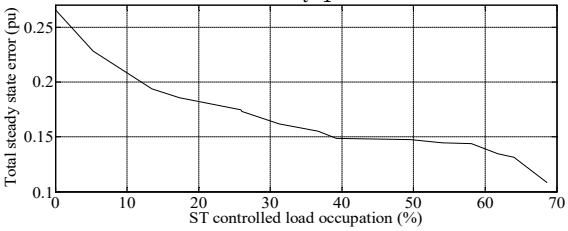

Fig. 10. Total voltage steady state error with the increase of ST controlled load in IEEE 39-bus system

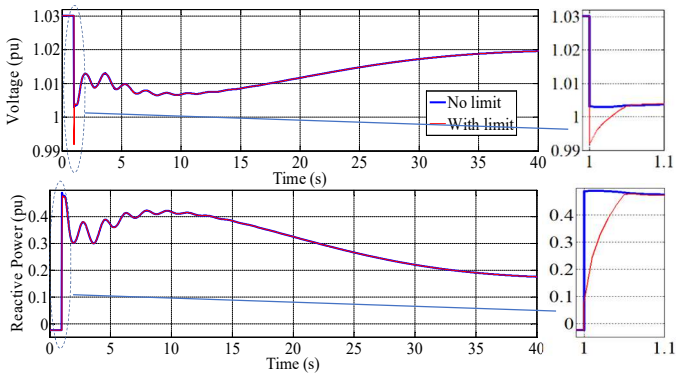

Fig. 11. The comparison of the controlled ST with/without limit

B. *Scenario 2*

In this Scenario, we focus on the influence of the converter power limit on the flexible demand control. Only the load on bus 3 ($P_L = 3.2$ $Q_L = 0.024$) is replaced by the ST controlled load. The converter power limit S_{ST} in (9) is set to 3.221, which means it is exactly at its maximum initially l. Fig. 11 displays the voltage and reactive power in bus 3 under the situations with and without a power rating limit imposed on the ST .

From Fig. 11, it can be seen that the converter power limit rarely affects the flexible demand performance on the voltage. This is because the voltage-reactive power droop gain computed from (12) is small and the active power reduction provides the space for the reactive power compensation. The main impact is during the transient (see zoom in plots), when the active power has not reduced, while the voltage has already dropped. In this case, the insufficient reactive power compensation makes the voltage nadir lower when the ST power limit is imposed.

V. Conclusion

Under the proposed flexible demand control, the ST could actively control the demand to support the frequency dynamically and statically, and moreover, support the voltage by reactive compensation. The resulting increased flexibility from demand under flexible demand control has the potential to facilitate increased renewable generation and may be preferable to shedding the load or maintaining reserve in back-up generators.

Acknowledgment

This work is part of Energy Systems Integration Partnership Programme ESIPP Project funded by the Science Foundation Ireland (SFI) with Grant Number SFI/15/SPP/E3125. And is part of the European Research Council under the European Union's Seventh Framework Programme (FP/2007-2013)/ERC Grant Agreement 616344 HEART. Muyang Liu and Federico Milano are supported by SFI Investigator Programme, Grant No. SFI/15/IA/3074.

References

[1] H. Beck and R. Hesse, "Virtual Synchronous Machine," 2007 9th International Conference on Electrical Power Quality and Utilisation, Barcelona, Spain, 9-11 October, 2007, 6 pp.

[2] O. Mo, S. Acro and J. Suul, "Evaluation of Virtual Synchronous Machines with Dynamic or Quasi-Stationary Machine Models", IEEE Transactions on Industrial Electronics, Vol. 64, no. 7, Jul. 2017.

[3] J. Chen, M. Liu, C. Loughlin, F. Milano and T. Donnell, "Modelling, Simulation and Hardware-in-the-Loop Validation of Virtual Synchronous Gnerator Control in Low Inertia Power System," 2018 Power Systems Computation Conference (PSCC), Dublin, Ireland, 11-15th, June, 2018.

[4] Q.-C. Zhong, P.-L. Nguyen, Z. Ma, and W. Sheng, "Self-synchronized synchronverters: Inverters without a dedicated synchronization unit," IEEE Trans. Power Electron., vol. 29, no. 2, pp. 617-630, Feb. 2014.

[5] S. Arco, J. A. Suul and O. B. Fosso, "A Virtual Synchronous Machine implementation for distributed control of power converters in Smart Grids," Electric Power Systems Research, Vol. 122, pp. 180-197, May 2015.

[6] Y. Ma, W. Cao, L. Yang, F. Wang and L. Tolbert, "Virtual Synchronous Generator Control of Full Converter Wind Turbines With Short-Term Energy Storage", IEEE Transactions on Industrial Electronics, Vol. 64, issue 11, pp. 8821-8831, Nov. 2017.

[7] W. Im, C. Wang, W. Liu, L. Liu and J. Kim, "Distributed Virtual Inertia Based Control of Mutiple Photovoltaic Systems in Autonomous Microgrid," IEEE/CAA Journal of automatic sinic, vol. 4, no. 3, Jul. 2017.

[8] R. Alzola, G. Gohil, L. Mathe, M. Liserre and F. Blaabjerg, "Review of Modular Power Converters Solutions for Smart Transformer in Distribution System," Energy Conversion Congress and Exposition (ECCE), 2013 IEEE Denver, CO, USA. 15-19 Sept, 2013, p. 380-387.

[9] X. Gao, G. Carne, M. Liserre and C. Vournas, "Increasing integration of Wind Power in Medium Voltage Grid by Voltage Support of Smart Transformer," WindEurope Summit 2016, Hamburg, Sept. 2016.

[10] G. De Carne, M. Liserre and C. Vournas, "On-Line Load Sensitivity Identification in LV Distribution Grdis," IEEE Transactions on Power Systems. Vol. 32 No.2 March 2017.

[11] J. Chen, C. Loughlin and T. Donnell, "Dynamic Demand Minimization using a Smart Transformer," 43rd Annual Conference of the IEEE Industrial Electronics Society (IECON), Beijing, China, 29 Oct.-01 Nov. 2017.

[12] G. Carne, G. Buticchi, M. Liserre and C. Vournas, "Load Control Using Sensitivity Identification by means of Smart Transformer," IEEE Transactions on Smart Grid, 3 Oct. 2016.

[13] M. Wesenbeeck, S. Haan, P. Varela and K. Visscher, "Grid tied converter with virtual kinetic storage," PowerTech, 2009 IEEE Bucharest, Romania, 28 Jun.-2 Jul. 2009.

[14] Copper Development Association "Voltage Disturbances Standard EN 50160- Voltage Characteristics in Public Distribution Systems", Power Quality Application Guide, July 2004.

[15] EirGrid, "EirGrid Grid Code Version 6.0," 22 July 2015.

[16] EirGrid and SONI, "DS3: Rate of Change of Frequency (ROCOF) Workstream," 2011.

[17] M. Tsili and S. Papathanassiou, "A review of grid code technical requirements for wind farms," IET Renewable Power Generation, vol. 3, Iss. 3, pp. 308-332, 2009.

[18] K. Mckenna and A. Keane, (2014) "Discrete Elastic Residential Load Response under Variable Pricing Schemes," Innovative Smart Grid Technologies Conference Europe (ISGT-Europe), 2014 IEEE PES, Istanbul, Turkey, Oct. 12-15, 2014.

[19] I. Ibrahim, V. Rigoni, C. Loughlin, S, Jasmin and T. Donnell, "Real-time Simulation Platform for Evaluation of Frequency Support from Distributed Demand Response," Cigre Symposium Dublin 2017. Paper 162.

[20] M. Khan, A. Milani, A. Chakrabortty, and I. Husain, "Dynamic Modeling and Feasibility Analysis of a Solid-State Transformer-Based Power Distribution System," IEEE Trans. Industry Applications, Vol. 54, No. 1, Jan/Feb. 2018.

[21] F. Milano, Power System Modelling and Scripting, Springer, London, August 2010.

[22] F. Milano, "A Python-based Software Tool for Power System Analysis," IEEE PES General Meeting, Vancouver, Canada, 21-25 July 2013.